

A 15-year climatology of stratosphere-troposphere exchange with a Lagrangian particle dispersion model:

1. Methodology and validation

P. James, A. Stohl, C. Forster, and S. Eckhardt

Department of Ecology, Technical University of Munich, Freising-Weihenstephan, Germany

P. Seibert and A. Frank

Institute of Meteorology and Physics, University of Agricultural Sciences, Vienna, Austria

Received 10 June 2002; revised 12 September 2002; accepted 13 September 2002; published 27 February 2003.

[1] The Lagrangian particle dispersion model, FLEXPART, which includes additional parametrizations for transport by subgrid-scale convection and turbulent eddies, is employed to investigate stratosphere-troposphere exchange (STE), based on 15 years of ECMWF global atmospheric reanalysis data (ERA-15). The model was initialized with 500,000 particles, distributed randomly throughout the atmosphere, and these were subsequently advected continually over the reanalysis period. The methodology employed in FLEXPART, allowing various age properties and pathways of air masses to be traced permanently on a very wide range of timescales, is described in detail. Empirical validation of the model results is presented. It is shown that typically more than 95% of the mass of the troposphere at any one time has been in the stratosphere within the preceding year, emphasizing the significance of STE. Cross-tropopause fluxes reveal regions of mean downward net flux in the subtropics flanked by mean upward net flux in the tropics and, more weakly, in the polar regions. Estimates of the mean net downward cross-tropopause flux in the northern extratropics agree well with other studies but are shown to be highly sensitive to the choice of latitude at which the extratropics are defined to begin. The mean age of tropospheric (stratospheric) air in the stratosphere (troposphere) is derived and shown to be somewhat underestimated, especially for tropospheric air at higher levels of the stratosphere, due largely to deficiencies in the vertical resolution of the ERA-15 stratosphere. *INDEX TERMS:* 0341 Atmospheric Composition and Structure: Middle atmosphere—constituent transport and chemistry (3334); 3309 Meteorology and Atmospheric Dynamics: Climatology (1620); 3334 Meteorology and Atmospheric Dynamics: Middle atmosphere dynamics (0341, 0342); 3362 Meteorology and Atmospheric Dynamics: Stratosphere/troposphere interactions

Citation: James, P., A. Stohl, C. Forster, S. Eckhardt, P. Seibert, and A. Frank, A 15-year climatology of stratosphere-troposphere exchange with a Lagrangian particle dispersion model: 1. Methodology and validation, *J. Geophys. Res.*, 108(D12), 8519, doi:10.1029/2002JD002637, 2003.

1. Introduction

[2] Stratosphere-troposphere exchange (STE) is an essential element of the three-dimensional global atmospheric circulation, having a central impact on mean atmospheric chemistry budgets in both stratosphere and troposphere. The eventual dispersion of boundary layer pollutants into the stratosphere, and the intrusion of stratospheric ozone into the lower atmosphere are just two examples driven by STE flows. Indeed, STE has many facets, includes many subordinate areas of research, and involves interactions on a very wide range of timescales. As such, any study wishing to summarize STE from a climatological point of view needs to appreciate the broad nature of the term and must

challenge competing viewpoints which attempt to limit discussion of STE to some subset of the whole.

[3] The simplest way to encapsulate STE is to think of it in terms of cross-tropopause flux alone (see the comprehensive review of STE by Holton *et al.* [1995], discussing the various methods used to define it). This definition, however, can be misleading, since it does not take the subsequent paths of air masses crossing the tropopause into account [Stohl *et al.*, 2003]. In a particular case, very large instantaneous cross-tropopause fluxes into the troposphere may be observed, but if the air mass trajectories result in a subsequent rapid return into the stratosphere without mixing into the troposphere, the event will be of little significance for tropospheric chemistry. Clearly much more significant are cases in which stratosphere-to-troposphere transport (here specifically referred to as STT to distinguish it from the general term STE, which refers nonspecifically to exchange in either direction) parcels

intrude deeply into the troposphere and have subsequently long residence times there. These parcels will eventually mix with tropospheric air and thereby contribute to the chemical budget of the troposphere.

[4] Deep intrusions of stratospheric air into the troposphere are often associated with tropopause folds related to cyclogenesis in the middle latitudes [e.g., *Browning*, 1997] or quasi-permanent tropopause folds in the subtropics [*Sprenger et al.*, 2003]. While the initial intrusion takes place rapidly, on timescales of synoptic baroclinic development, the principle of dissipation ensures that much of the descending air mass will reside subsequently for a much longer period of time in the troposphere. The arrival in such cases of stratospheric air rich in ozone has thus a strong impact on the oxidizing capacity of the troposphere [*Ebel et al.*, 1991], especially considering that as much as 40% of tropospheric ozone may have a stratospheric origin [*Roelofs and Lelieveld*, 1997].

[5] Similar arguments apply to flows in the opposite direction, from the troposphere upwards into the stratosphere, referred to as troposphere-to-stratosphere transport (TST). In the extratropics TST flows are frequent [*Vaughan and Timmis*, 1998], but also predominantly shallow and transient in nature since tropospheric air cannot penetrate quickly or deeply into the stratosphere due to the high static stability and the large-scale descent in the lower stratosphere [*Holton et al.*, 1995]. The most effective TST penetration occurs above the tropical convergence zone where a slow mean ascent is observed [*Plumb*, 1996; *Mote et al.*, 1996] and where convective plumes may top 20 km. In such cases, embedding in the Brewer-Dobson circulation [*Brewer*, 1949], which subsequently transports the air into the extratropical stratosphere [*Waugh*, 1996], can result in a portion of the TST air staying in the stratosphere for up to several years before its eventual return [e.g., *Andrews et al.*, 2001; *Reithmeier*, 2001], having been thoroughly mixed in the mean time with other stratospheric air. Hence, while instantaneous TST mass fluxes across the tropopause may be large in the extratropics, it is the slow TST fluxes, initialized in the tropics, which play the greatest role in stratospheric chemistry, emphasizing again the need to examine both the depth and the timescales of exchange, to gain a meaningful appreciation of STE as a whole.

[6] Foundational estimates of mean net cross-tropopause mass fluxes, which serve as a basis for validating new studies, include those of *Juckes* [1997, 2000] who looked at the mean meridional mass flux based on quasi-geostrophic theory and *Appenzeller et al.* [1996] who estimated the hemispherically integrated monthly net downward flux in the extratropics based on the mass of the lowermost stratosphere and the annual cycles of the residual mean circulation. The drawback of such estimates, quite apart from their not addressing the question of depth of exchange, is that they do not account for the highly episodic nature of STE either [*Appenzeller and Davies*, 1992], which is most notable in the extratropics associated with strong meso-scale perturbations of the tropopause. This is especially important in relation to mean residence times, for which climatological mean fluxes can give little indication. In light of this, the traditional method of estimating actual STE fluxes and locations is the Wei method [*Wei*, 1987] using Eulerian diagnostics [e.g., *Hoerling et al.*, 1993; *Grewe and Dameris*, 1996; *Siegmund et al.*, 1996]. However, the Wei approach proves to be rather

inaccurate, due to cancellations between large numerical terms and high sensitivity to inaccuracies in the underlying data [*Wirth*, 1995; *Wirth and Egger*, 1999; *Gottelman and Sobel*, 2000], to provide consistent STE flux estimates, especially if gross upward and downward fluxes are compared [*Kowol-Santen et al.*, 2000]. As a result, there has been poor agreement of results from different studies.

[7] To incorporate depth of exchange and the residence time aspect into an STE assessment, the Lagrangian approach [e.g., *Wernli and Davies*, 1997] is of invaluable benefit. A classical application of Lagrangian ideas is the production of airstream trajectories based on observational wind field data. An early example of such a study, in which the material change of potential vorticity (PV) along the trajectories must be estimated, is that of *Danielsen* [1968]. Recently, *Stohl* [2001] produced a one-year climatology of northern hemisphere airstreams, of which STT and TST flows are a subset, using a Lagrangian trajectory model based on operational ECMWF analysis data. Similarly, *Wernli and Bourqui* [2002] produced a comparable climatology, but looking specifically at STT and TST flows, using a different Lagrangian model. These showed that cross-tropopause mass flux estimates depend critically on the timescales considered as well as on the definition of the tropopause region, particularly on its thickness.

[8] Notwithstanding the advantages of a trajectory approach, such models still have specific limitations which need to be addressed. First, residence times of exchange flows which can be measured are limited by the length of the calculated trajectories, which are usually cut off after 7 to 10 days at the very most. Second, it is known that deep cumulus convection plays an important role for rapid vertical transport in the tropics as well as in the extratropics in the summer half-year and also occurs during the decay of cut-off lows throughout the year. Yet, this is not explicitly resolved in the ECMWF data sets. Thirdly, stratospheric air brought down deep into the troposphere may eventually be mixed to the surface by boundary layer turbulence, which is also not accounted for in trajectory calculations.

[9] A Lagrangian approach which fills these gaps is particle dispersion modeling in which particles act as tracers for specific properties of the air masses they represent while being continually advected. In this paper, the Lagrangian particle dispersion model FLEXPART [*Stohl et al.*, 1998; *Stohl and Thomson*, 1999] is integrated over the ECMWF reanalysis data set period (ERA-15) to produce a comprehensive 15-year climatology of STE, presenting its typical magnitudes, timescales, seasonality and spatial and inter-annual variability. Using FLEXPART, estimates of residence times of exchange flows are limited only by the total length of the model integration itself, in this case 15 years, allowing for the first time an explicit assessment of residence times on seasonal and even interannual timescales. Hence, our results compliment and extend the findings of *Sprenger and Wernli* [2003], who employ a comparable Lagrangian approach to examine the climatological aspects of STT and TST trajectories, traced for up to 4 days after crossing the tropopause. In chapter 2, the FLEXPART model setup and input data are described. Climatological aspects of STE fluxes and mass distributions useful for validation against results in other literature are detailed in chapter 3 while a summary is drawn in chapter 4.

Other findings relating to the mean climatology of STE and its seasonality are presented by *James et al.* [2003].

2. Model and Input Data Setup

[10] The stochastic Lagrangian particle model FLEXPART calculates the transport and dispersion of nonreactive tracers, driven by input model-level meteorological data which may be observational or derived from climate model simulations. FLEXPART has been validated with data from large-scale tracer experiments [*Stohl et al.*, 1998] and performs well in comparison with other models [*Meloen et al.*, 2003]. It has been used for studying the intercontinental transport of ozone [*Stohl and Trickl*, 1999], the advection of Canadian forest fire emissions to Europe [*Forster et al.*, 2001] and the dispersion of aircraft emissions in the stratosphere [*Forster et al.*, 2003], for example. Specific validation of STT in FLEXPART has been performed [*Stohl and Trickl*, 1999; *Stohl et al.*, 2000] and has been compared with measurement data during case-studies of stratospheric intrusions [*Cristofanelli et al.*, 2003].

[11] For this study, the 15-year ECMWF reanalysis data set (ERA-15 [*Gibson et al.*, 1997]) was deployed, using a global data coverage for the period 1979 to 1993 with a 6-hourly analysis frequency. All 31 available vertical model levels are used, of which the highest lies at 10 hPa, with a $1^\circ \times 1^\circ$ resolution in the horizontal derived from spectral fields with a resolution of T106. The fields specifically required by FLEXPART include fully 3-dimensional wind, temperature and specific humidity, stored on model-levels, as well as surface fields used for FLEXPART parametrizations, such as turbulence and convection. ERA-15 is the most comprehensive and accurate long-term homogeneous meteorological data set currently available from ECMWF, at least up to the tropopause region. However, it has a model top at 10 hPa and a coarse vertical resolution in the stratosphere (the uppermost model levels are at 110, 90, 70, 50, 30, and 10 hPa) and enhanced diffusion is applied close to the model top, which affects the accuracy of stratospheric winds. ERA-15 is too warm above 100 hPa in the tropics, compared to measurement data [*Pawson and Fiorino*, 1998a] and it underestimates the amplitude of the quasi-biennial oscillation (which is even unrealistic at 10 hPa) [*Pawson and Fiorino*, 1998b] for which a high vertical resolution of the order of 500 m would be needed in the stratosphere [*Baldwin et al.*, 2001]. Furthermore, the cross-equatorial mass fluxes above 100 hPa cannot be regarded wholly accurate [*Pawson and Fiorino*, 1998a]. These points suggest that the Brewer-Dobson circulation is also not likely to be realistically captured by ERA-15. This can also be inferred from results by *Rind et al.* [1999] who showed how reducing the vertical resolution of a general circulation model in the stratosphere to that typical for the ERA-15 data results in a significantly weaker Brewer-Dobson circulation. Therefore, we focus on STT and on extratropical TST, and do not study transport features at higher stratospheric levels.

[12] The tropopause is defined in FLEXPART as a dynamical tropopause polewards of 30° and a thermal tropopause equatorwards of 20° . Between these latitudes, the two definitions are linearly interpolated. The dynamical

tropopause is represented by the PV surface of 2 pvu (where $1 \text{ pvu} = 10^{-6} \text{ K m}^2 \text{ kg}^{-1} \text{ s}^{-1}$), in common with many other studies [e.g., *Holton et al.*, 1995; *Appenzeller et al.*, 1996], while the thermal tropopause is the lower boundary of a layer with a thickness of 2 km, in which the temperature gradient is lower than 2 K km^{-1} [*Hoinka*, 1997]. The dynamical tropopause definition polewards of 30° allows for the existence of a multiple tropopause in a vertical profile and thus for possible tropopause folds.

[13] The FLEXPART integration was set up for starting on 1 January 1979 with 500,000 particles initialized with a random but homogeneous distribution throughout the global atmosphere, in proportion with air density. The number of particles used was found to be an optimum between the need for a sufficient level of derived statistical significance and the amount of model integration time required for such a calculation. The particles were then continually advected throughout the 15-year integration with no sink or source of new particles. During the integration, stochastic fluctuations, obtained by solving the Langevin equations [*Stohl and Thomson*, 1999], are superimposed on the grid-scale winds to represent transport by turbulent eddies. In the atmospheric boundary layer (ABL) turbulence is parametrized in detail, but in the free troposphere it is simply dependent on wind shear. As in other models, turbulence in the free troposphere is a poorly parametrized process, with large uncertainties in both magnitude and location and time of occurrence.

[14] The large-scale effects of convection, such as the strong ascent at the intertropical convergence zone or line convection in warm conveyor belts, are reproduced in ECMWF data. However, smaller scale convective cells are not resolved. To counter this problem, such subgrid-scale deep convection is parametrized in FLEXPART using the scheme of *Emanuel and Zivkovic-Rothman* [1999]. The scheme utilizes the grid-scale temperature and humidity data, providing a uniform treatment of all moist convection types (i.e., shallow to deep). A displacement matrix is calculated for every model column and displacement probabilities for individual particles are derived. The scheme was tuned such that it best reproduces the convective precipitation fields that were generated on-line by the ECMWF model and are available in the ERA-15 data set, in order to be as consistent as possible with the driving meteorological model. The implementation and testing of the scheme has been described by *Seibert et al.* [2001]. Turning on the convection scheme in FLEXPART has only a moderate effect on results in the extratropics. However, it has a significant influence in the tropics, helping to drive more realistic transport amplitudes than the raw ECMWF data could account for.

[15] During the subsequent integration, each particle traces 5 different properties of the air, which are carried by respective time flags. The 5 properties (species) represent different source layers of the atmosphere, defined primarily by potential vorticity (PV). These 5 species are listed in Table 1. The first two are for stratospheric air. The first of these, defined by $PV > 4 \text{ pvu}$, is for air sourced above, and not including, the stratospheric part of the tropopause region (TPR). Note that, for the purposes of this study, the TPR is considered to be the region immediately above and below the tropopause, bounded between the 4 pvu and 1 pvu

Table 1. Definitions of the Five Tracer Species Used in the FLEXPART Model Integration^a

Species	Definition	Description
1	PV > 4 pvu (and $z > 1000\text{m}$)	Stratospheric air (not including TPR)
2	PV > 2 pvu (and $z > 1000\text{m}$)	All stratospheric air
3	PV > 1 pvu (and $z > 1000\text{m}$)	Stratospheric and TPR air
4	PV < 2 pvu	Tropospheric air
5	Below ABL top	Boundary Layer air

^a z is the height above local orography.

surfaces, respectively. The TPR is thus the region within which transient, quasi-reversible cross-tropopause flows are bounded, as opposed to deep, irreversible STE flows which extend beyond the TPR. Note also that the upper TPR is not coincident with the lowermost stratosphere, defined traditionally as the region bounded above by the 380 K isentrope [Holton *et al.*, 1995]. The second species is for all stratospheric air, including the TPR layer directly above the tropopause (PV > 2 pvu). The third species further extends the definitions of the first two by also including the TPR layer below the tropopause (hence PV > 1 pvu). This extension of the species definitions to include separate treatments of the TPR is important for allowing questions about the depth and significance of the layer over which STE typically occurs to be addressed adequately. Additionally, these first 3 species are also required to be sourced at least 1 km above the height of the local orography. This is necessary since intense surface cooling can result occasionally in local PV values exceeding 2 pvu in the ABL over topography, even though stratospheric or TPR air is clearly not involved. The fourth species exclusively represents tropospheric air (PV < 2 pvu) and the last species boundary layer air sourced below the ABL top. The ABL depth itself is determined using the parametrization of *Vogelezang and Holtslag* [1996] which works for both stable and convective ABLs.

[16] Note that the PV definitions of these surfaces are applied only polewards of 30°. As described earlier for the tropopause definition, corresponding thermal definitions were used equatorwards of 20°. These were selected such that, on average, thermal and dynamical definitions agree best in the latitude belt 20°–30°, where the two surfaces were linearly interpolated. The 2 pvu surface fits with the WMO definition of the thermal tropopause and analogous criteria were used for the 4 pvu and 1 pvu surfaces respectively.

[17] Whenever a particle leaves a source level for one or more of the species, the time flag (clock) for that species on that particle begins counting. Similarly, when a particle enters a source level for a species, the clock for that species and particle is reset to zero. Hence, residence times of air masses away from their source levels, until their (eventual) return, can be determined. To reduce the total residence time information into a manageable data set and allow a convenient statistical assessment of typical residence times to be made, the residence times are boxed into 14 age classes, as listed in Table 2. These range from less than 6 hours to more than one year. Older age classes would have been less useful because of the poor representation of the Brewer-Dobson circulation in the ERA-15 data. A 15th age class is also used for particles with species which have not yet been

initialized, having never yet entered a certain layer. Species indeed become initialized on the vast majority of particles within the first two years of integration. For example, at the end of the first year (1979), approximately 4.3% of the mass of the troposphere had not yet been in the stratosphere. By the end of the second year this fraction had fallen to 0.15% and had fallen further to just 0.004% by the end of the third year. By 1993, all particles had been at least once in the stratosphere.

[18] The model output is produced on a monthly mean basis. First, mixing ratios and concentrations of each species and for each age class are produced on a 3D grid. To achieve this, the particle trajectory positions are not stored permanently themselves, but the output fields are computed every model time step of 900 s and subsequently averaged. The output data is separated into stratospheric and tropospheric results, by operationally determining whether the particle positions are currently above or below the tropopause (independent of source), thus contributing its tracer data to a stratospheric or to a tropospheric results data set. This separation is necessary since the tropopause height fluctuates considerably and so it would be otherwise hard to interpret the meaning of average tracer concentrations near the height of the mean tropopause. The output grid was optimally chosen to have a 3° latitude by 5° longitude horizontal resolution and 14 height levels in the vertical, ranging from 500 m to 27 km above local orography, the vertical interval increasing stepwise with height. Explicitly computed mean ages of each species, separated into stratospheric and tropospheric results, are also produced on this output grid.

[19] Furthermore, mass fluxes of the tracers as a function of age class across a number of control surfaces are produced on the horizontal axes of the above grid. Twelve control surfaces are used: 6 pressure surfaces (850, 700, 500, 300, 200, 100 hPa), 4 PV surfaces (1, 2, 4, 10 pvu), the ABL top and 500m above the local orography. The mass fluxes are separated into upwards, downwards and net fluxes, while each of these total mass fluxes is further separated into turbulent, grid-scale, convective and local tendency components, the latter being due to altitude changes of the control surface.

[20] During the integration the particle distribution was frequently sampled to test for homogeneity. This confirmed that the particles remain very homogeneous throughout, with no tendency for any shift in mean altitude or meridionality to occur. After completing the integration, the final set of 168 monthly mean data sets was averaged as a whole to produce a general climatological picture of STE. Note that the year 1979 is excluded from the results since the populations of older age classes in particular require a certain spin-up time before reaching equilibrium. Various subsets of the data were also averaged to tackle questions relating to seasonality,

Table 2. Age Classes Used in the FLEXPART Model Integration

Age Class	Residence Time, hours or days	Age Class	Residence Time, days	Age Class	Residence time, days
1	0–6 hours	6	3–4	11	20–40
2	6–12 hours	7	4–6	12	40–90
3	12–24 hours	8	6–8	13	90–365
4	1–2 days	9	8–10	14	>365
5	2–3 days	10	10–20	15	Not yet initialized

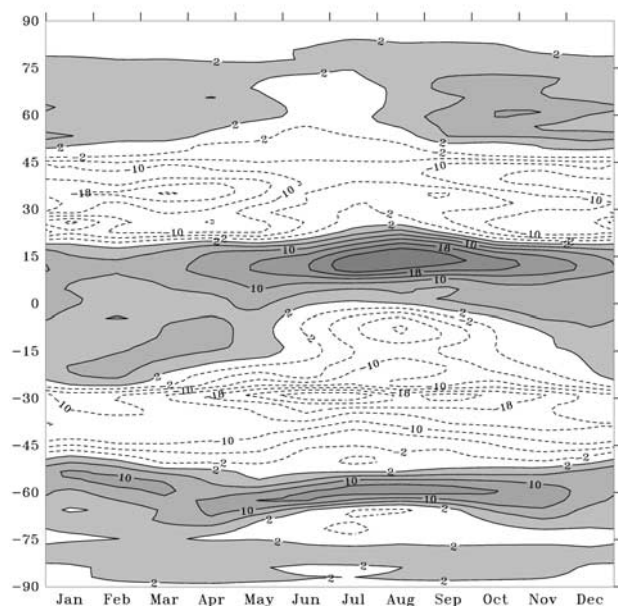


Figure 1. Mean seasonal cycle of the zonal-mean net cross-tropopause flux as a function of latitude in units of $10^8 \text{ kg s}^{-1} \text{ deg}^{-1}$. Positive values (shaded) represent upward net flux, negative contours are dashed.

variability, and relationship to aspects of the atmospheric circulation. Some general results which serve to validate the output are presented in the next section.

3. Validation

[21] Before specific aspects of the climatology itself can be discussed, it is of paramount importance to validate first some basic output quantities against results elsewhere in the literature, to confirm that the model integration has performed as intended. A useful global quantity is the mean net cross-tropopause mass flux, as defined by the 2 pvu surface. The climate mean seasonal cycle of this net flux is shown in Figure 1. A number of aspects of this picture can be anticipated from a knowledge of the general circulation, such as the mean net upward flux above the inter-tropical convergence zone (ITCZ), especially during the northern summer when the ITCZ shifts northwards over regions where a greater percentage of land surface (than further south) induces more intense convective cells. Over the subtropics and midlatitudes up to about 50°N and 50°S , respectively, a mean net downward flux is seen, where midlatitude troughs extend towards the subtropics. Polewards of these regions, by contrast, a mean net upward flux is seen, typically associated with warm conveyor belts, especially those which stream polewards and westwards of blocking anticyclones.

[22] The presence of mean net upward fluxes across the tropopause in polar regions may seem to contradict the traditional view of the Brewer-Dobson circulation as proposed by Brewer [1949], which envisages air moving into the stratosphere in the tropics and descending into the troposphere in the extratropics. However, more recent calculations of air motions relative to PV surfaces [Hoerling *et al.*, 1993; Grewe and Dameris, 1996] and theory pre-

sented by Juckes [1997] have shown that such a mean net upward flux can be anticipated on the polar side of the baroclinic zone, whereby in some cases trajectories associated with this upward flux may in fact be descending in altitude, but more slowly than the local slope of the tropopause which they subsequently cross into the stratosphere. Sprenger and Wernli [2003] also find a region of mean net upward cross-tropopause fluxes in the northern hemisphere, albeit only very weakly so and limited to the Arctic. Furthermore, their latitudes of maximum net downward flux and of the crossover lines of zero net flux in the subtropics and towards the polar regions are all typically about 5° further north than in our results. Their findings are based, however, on only the subset of cross-tropopause trajectories whose subsequent residence times exceed 96 hours, whereas our estimates utilize all trajectories, including those of a transient nature of which there are a substantial number [see James *et al.*, 2003]; and they do not use parametrizations for convection and turbulence.

[23] Figure 1 further indicates that there are considerable differences in mean net flux amplitudes between the two hemispheres. The regional mean net downward flux in the southern subtropical to midlatitudinal belt (21° to 51°S) is $2.8 \times 10^{10} \text{ kg s}^{-1}$ compared to $2.4 \times 10^{10} \text{ kg s}^{-1}$ for the equivalent northern hemisphere region. An even greater difference is seen over the respective polar regions where the mean net upward flux in the southern hemisphere of $1.7 \times 10^{10} \text{ kg s}^{-1}$ is much larger than in the northern hemisphere ($1.1 \times 10^{10} \text{ kg s}^{-1}$).

[24] The mean total cross-tropopause flux over the northern extratropics in winter (DJF), derived from the values plotted in Figure 1 can be compared with other estimates summarized by Gettelman and Sobel [2000, Figure 8]. If we define the extratropics as starting at 28°N , as they have done, our results give an estimate of almost exactly $100 \times 10^8 \text{ kg s}^{-1}$ net downward flux, which lies just below the comparable budget estimates of Gettelman and Sobel [2000] and Appenzeller *et al.* [1996], which are about 20% and 40% higher respectively. However, the estimate is clearly highly sensitive to the definition of the extratropical boundary. In our findings, the mean net downward fluxes in the subtropics continue to around 21°N , which would appear to be a better definition of the boundary for these purposes. Using this latter definition, our total net flux estimate increases to $165 \times 10^8 \text{ kg s}^{-1}$, somewhat higher than both budget estimates.

[25] To validate the seasonal cycle of the extratropical net cross-tropopause fluxes our fluxes for the years 1992 and 1993 are compared in Figure 2 with those estimated for this period by Appenzeller *et al.* [1996, Figure 8]. Although the annual mean net flux and the phase of the seasonal cycle are rather similar to our own, the amplitude of our seasonal cycle and month-to-month variability is significantly larger. During some summer months, there is even net TST, in contrast to the Appenzeller *et al.* study. This indicates that budget estimates fail to resolve sufficiently those seasonally varying aspects of the general circulation important for variations in the mean net fluxes.

[26] The year-to-year robustness of the model integration and the ERA-15 data upon which it is based is illustrated in Figure 3, which shows the interannual variations of the net cross-tropopause fluxes, averaged over the five intrinsic

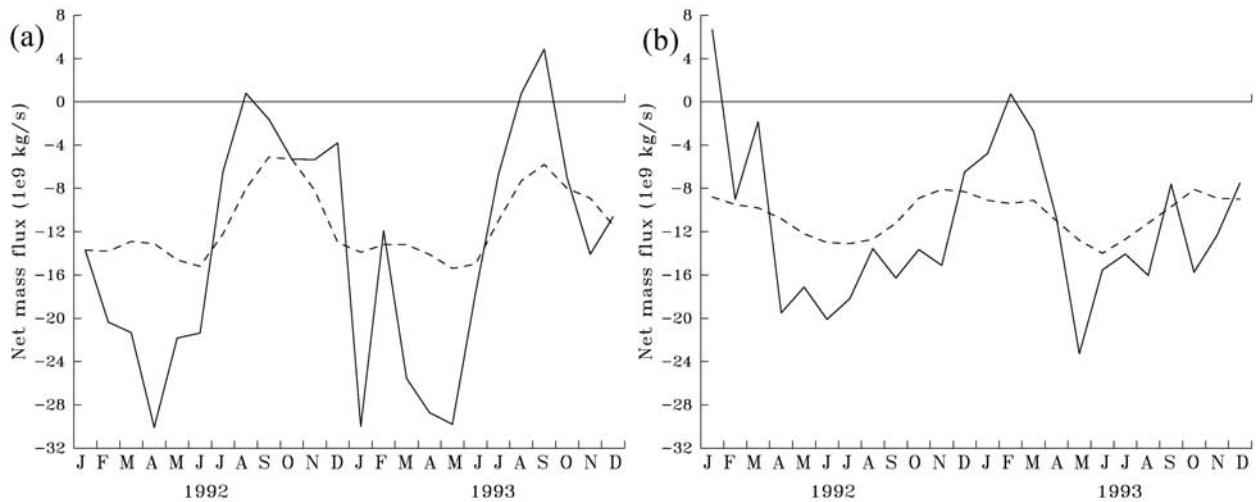


Figure 2. Monthly mean total net mass transports (solid curves) across the extratropical tropopause in 10^9 kg s^{-1} during 1992 and 1993 for (a) the northern hemisphere (21°N – 90°N) and (b) the southern hemisphere (21°S – 90°S). The dashed curves show the equivalent values estimated by *Appenzeller et al.* [1996].

zonal regions of the globe as defined by the mean sign of the net fluxes, respectively. The interannual variability of these net flux estimates, which is not insubstantial, is composed of a superposition of the intrinsic variability of the net flux magnitudes within each of the five regions and

the effect of meridional shifts of the zonal mean position of these regions; the latter evidenced by considerable anticorrelations in net flux contributions from adjacent regions. Notwithstanding this latter effect, the interannual variability has a generally lower magnitude than the respective sea-

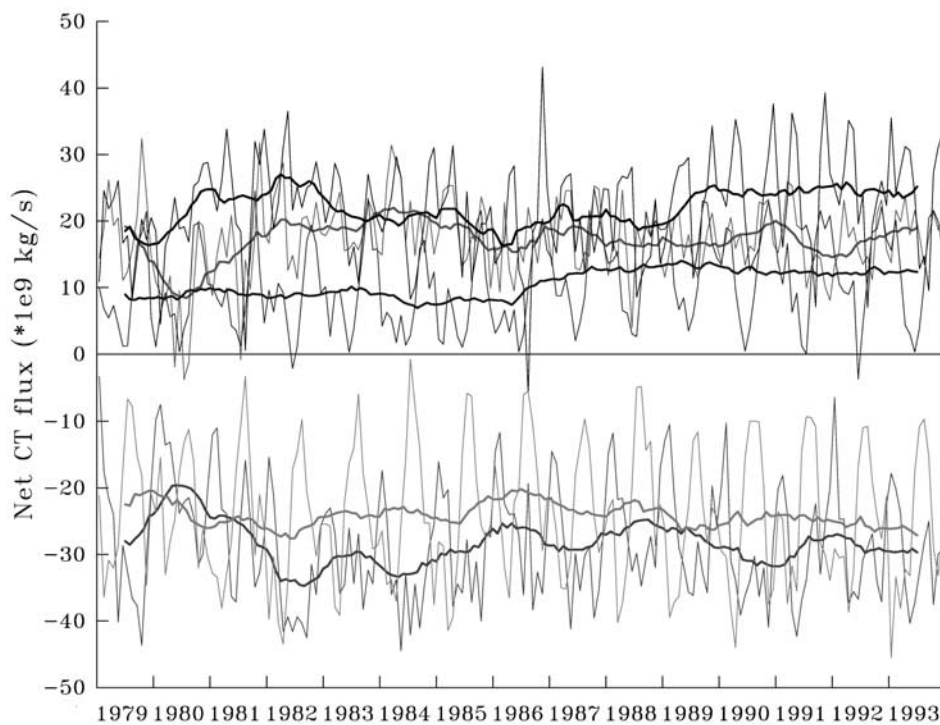


Figure 3. Meridionally integrated monthly mean zonal-mean net cross-tropopause fluxes, units 10^9 kg s^{-1} , with 12-month running means (thicker lines) for 1979 to 1993, averaged over 5 latitude bands: 51°N – 90°N (blue), 21°N – 51°N (green), 21°S – 21°N (black), 51°S – 21°S (red), 90°S – 51°S (violet). See color version of this figure at back of this issue.

Table 3. Relative Contributions of the Four Flux Components to the Total Flux in Percent, for Five Different Latitude Bands, Based on Annual Mean RMS of Upward and Downward Fluxes Across the 850 and 500 hPa Pressure Surfaces (Upper Table) and Across the 2 and 10 pvu PV Surfaces (Lower Table)^a

Region	850 hPa				500 hPa			
	G	T	C	L	G	T	C	L
51°N–90°N	10.7	87.0	1.5	0.8	89.8	2.1	1.5	6.6
21°N–51°N	9.1	88.7	1.8	0.4	61.0	34.0	2.5	2.6
21°S–21°N	13.1	81.8	4.1	1.0	76.9	6.9	11.5	4.6
51°S–21°S	9.4	87.8	2.2	0.6	84.9	9.2	1.5	4.5
90°S–51°S	8.3	87.9	2.8	1.0	87.1	2.0	2.2	8.7

Region	2 pvu				10 pvu			
	G	T	C	L	G	T	C	L
51°N–90°N	50.6	2.1	0.2	47.1	53.5	1.7	0.0	44.8
21°N–51°N	59.5	1.6	0.4	38.6	55.8	1.6	0.1	42.6
21°S–21°N	63.7	1.4	1.6	33.2	43.7	2.1	0.9	53.3
51°S–21°S	53.8	1.4	0.3	44.6	51.2	1.4	0.0	47.3
90°S–51°S	48.5	1.9	0.3	49.4	53.2	1.8	0.0	45.0

^aG, grid-scale; T, turbulent; C, convective; L, local tendency.

sonal cycles. No significant trends can be detected, but the series for the region north of 51°N indicates a sudden jump to higher values during 1986, which coincides with changes in the satellite observing system that were noted previously to cause a discontinuity in the ERA-15 data set [Trenberth *et al.*, 2001; Källberg, 1997]. Other discontinuities in the ERA-15 data (e.g., one in 1989) were found by Trenberth *et al.* [2001], which possibly coincide with smaller discontinuities in our net STE fluxes. This renders trend studies of STE, based on ERA-15 data, unreliable. However, the time series appear robust enough to study the seasonality and interannual variability of STE.

[27] Another aspect of the model calculations which needs to be checked is that the mean relative contributions of the four component fluxes to the total flux are realistic. As shown in Table 3, the turbulent flux dominates strongly across the 850 hPa surface where considerable ABL turbulence is to be expected. Here, the convective flux contribution is typically around a quarter of the grid-scale flux contribution, being almost twice as high in the tropics than elsewhere. Across the 500 hPa surface the grid-scale fluxes

dominate, while large turbulent fluxes are only found over major mountain ranges where the ABL may sometimes extend beyond this pressure level. In contrast to looking at pressure surfaces whose vertical motion is relatively negligible, the contribution from the local tendency term becomes far more significant for fluxes across PV surfaces, accounting for nearly one half of the total flux amplitudes at the 10 pvu surface. Here, well into the stratosphere, the turbulent flux contribution has dropped to less than 2% of the total while the convective fluxes are negligible, except perhaps in the tropics, where the Emanuel convection scheme [Emanuel and Zivkovic-Rothman, 1999] is capable of simulating detrainment from overshooting cumulo-nimbus tops. Note that although convective fluxes at 10 pvu are relatively small, they are nevertheless important, as they deposit plumes of lower tropospheric air directly into the stratosphere.

[28] A useful statistic for describing the mean distribution of STE air masses is the mean age of tracers outside of their respective source regions. Illustrative climate mean ages of STT air in the troposphere and TST air in the stratosphere are shown in Figure 4, respectively. As described in more detail James *et al.* [2003], most STT flows entering the troposphere penetrate no further than the upper troposphere. Deep STT reaching the lower troposphere becomes successively rarer with decreasing altitude so that the mean age of STT air increases with depth. The highest mean STT ages are of the order of 4 months in the tropics where the trade-wind circulations slowly gather old STT air originating in mid-latitude and subtropical deep intrusions.

[29] For TST flows on the other hand, the inherently high static stability of the stratosphere hinders rapid ascent of TST air masses. As a result, the mean age of TST air increases quickly with height. Nevertheless, a gradual entrainment of TST air into the slow Brewer-Dobson circulation does occur, transporting some of this air, which is typically injected into the stratosphere in the tropics above the ITCZ, towards the poles. The mean TST ages at about 18 km in the middle latitudes is about 500–600 days. Andrews *et al.* [2001] derive a somewhat higher mean age of about 2.5 years in the same region, based on carbon dioxide observations. They show that the age spectrum in this region is composed of two independent age distribu-

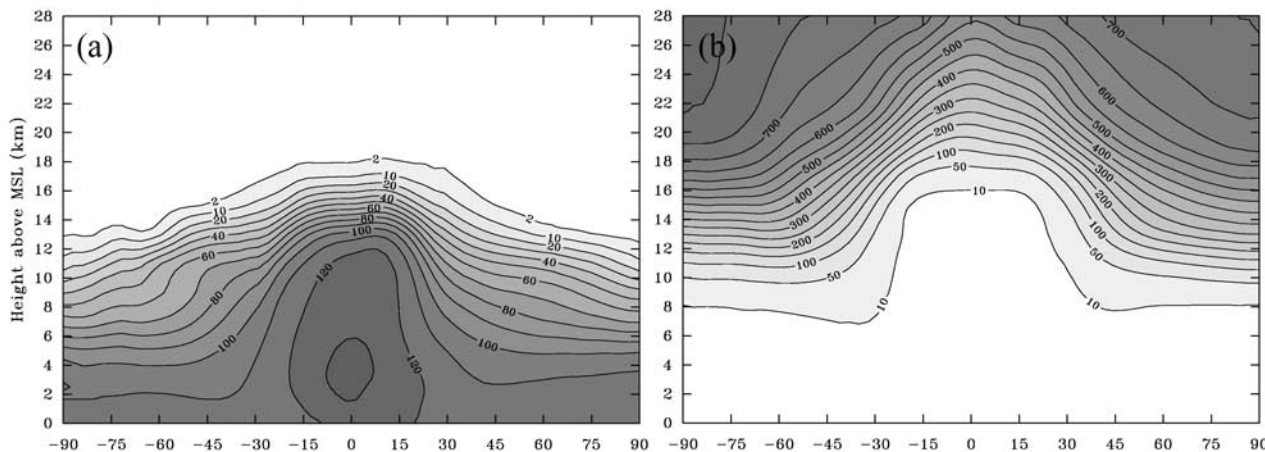


Figure 4. Latitude-height sections showing the zonally averaged mean age in days of (a) stratospheric (PV > 2) tracer in the troposphere and (b) the tropospheric (PV < 2) tracer in the stratosphere.

tions, one with a peak at less than half a year, the other with a peak at around 6 years, which is related to descent of aged air from the overworld. Similar mean ages were simulated by Reithmeier [2001] in a climate model simulation with a fully Lagrangian transport scheme and compared with SF₆ concentrations.

[30] Eluszkiewicz *et al.* [2000] have shown that age estimates are strongly sensitive to the choice of advection scheme, whereby semi-Lagrangian schemes typically underestimate ages the most. Nevertheless, such problems must always be borne in mind when deriving age-of-air estimates. Comparison with observational estimates suggests that, up to altitudes of about 20 km, our model estimates are fairly realistic, but at higher altitudes they underestimate the mean age considerably. Park *et al.* [1999], for example, shows that the mean age typically exceeds 8 years in the polar vortices at around 24 km altitude. Hence, it appears that the underestimate of mean age in our model in the lower stratosphere is largely caused by the severe underestimation of mean age in the uppermost regions of the reanalyzed stratosphere. This in turn appears to be due to the Brewer-Dobson circulation not being adequately captured by the ERA-15 data.

4. Summary

[31] A specially tuned version of the Lagrangian particle dispersion model, FLEXPART, has been employed to undertake a comprehensive study of STE, based on 15 years of ECMWF global atmospheric reanalysis data. The goal of this work is to produce a detailed climatology of STE, showing its typical amplitudes, timescales, seasonality and spatial and temporal variability, focussing in particular on deep and long-lasting exchange. Hence, a much broader view of STE than has previously been possible is enabled with this study. All the main findings relating to this climatology are presented by James *et al.* [2003]. In this first paper, the model setup and the experiment methodology employed, in which a large number of particles are traced permanently and globally, allowing various age properties and pathways of air masses to be assessed on a very wide range of timescales, has been described in detail. Then, in order to provide a solid foundation for discussing the STE climatology in part B, some aspects of net mass fluxes and distributions with respect to tracer age have been validated against other results in the literature.

[32] Typically more than 95% of the mass of the troposphere at any one time has been in the stratosphere within the preceding year, emphasizing the significance of STE. Cross-tropopause fluxes reveal regions of mean downward net flux in the subtropics flanked by mean upward net flux in the tropics and, more weakly, in the polar regions; this latter result being a relatively recent discovery. Estimates of the mean net downward cross-tropopause flux in the northern extratropics agree well with other studies but are shown to be highly sensitive to the choice of latitude at which the extratropics are defined to begin. The mean age of tropospheric (stratospheric) air in the stratosphere (troposphere) is derived and shown to be somewhat underestimated, especially for tropospheric air at higher levels of the stratosphere, due largely to deficiencies in the vertical resolution of the ERA-15 stratosphere.

[33] The validation results demonstrate that the model integration has performed as anticipated, yielding statistics which compare well with other studies, paving the way for the more detailed results of James *et al.* [2003].

[34] **Acknowledgments.** This research has been carried out as part of the STACCATO project (influence of Stratosphere-Troposphere exchange in A Changing Climate on Atmospheric Transport and Oxidation capacity), funded by the European Commission under contract no. EVK2-1999-00316 as part of the Fifth Framework Programme. The ECMWF and the German Weather Service (DWD) are also gratefully acknowledged for giving us access to the reanalysis atmospheric data sets. We thank the STACCATO community and H. Wernli in particular for valuable discussions.

References

- Andrews, A. E., *et al.*, Empirical age spectra for the midlatitude lower stratosphere from in situ observations of CO₂: Quantitative evidence for a subtropical “barrier” to horizontal transport, *J. Geophys. Res.*, *106*, 10,257–10,274, 2001.
- Appenzeller, C., and H. C. Davies, Structure of stratospheric intrusions into the troposphere, *Nature*, *358*, 570–572, 1992.
- Appenzeller, C., J. R. Holton, and K. H. Rosenlof, Seasonal variation of mass transport across the tropopause, *J. Geophys. Res.*, *101*, 15,071–15,078, 1996.
- Baldwin, M. P., L. J. Gray, and T. J. Tunkerton, The quasi-biennial oscillation, *Rev. Geophys.*, *39*, 179–229, 2001.
- Brewer, A. M., Evidence for a world circulation provided by the measurements of helium and water vapor distribution in the stratosphere, *Q. J. R. Meteorol. Soc.*, *75*, 351–363, 1949.
- Browning, K. A., The dry intrusion perspective of extra-tropical cyclone development, *Meteorol. Appl.*, *4*, 317–324, 1997.
- Cristofanelli, P., *et al.*, Stratosphere-troposphere transport: A model and method evaluation, *J. Geophys. Res.*, *108*, doi:10.1029/2002JD002600, in press, 2003.
- Danielsen, E. F., Stratospheric-tropospheric exchange based on radioactivity, ozone and potential vorticity, *J. Atmos. Sci.*, *25*, 502–518, 1968.
- Ebel, A., H. Hass, H. J. Jakobs, M. Laube, M. Memmesheimer, A. Oberreuter, H. Geiss, and Y.-H. Kuo, Simulation of ozone intrusion caused by a tropopause fold and cut-off low, *Atmos. Environ.*, *Part A*, *25*, 2131–2144, 1991.
- Eluszkiewicz, J., R. S. Hemler, J. D. Mahlman, L. Bruhwiler, and L. L. Takacs, Sensitivity of age-of-air calculations to the choice of advection scheme, *J. Atmos. Sci.*, *57*, 3185–3201, 2000.
- Emanuel, K. A., and M. Zivkovic-Rothman, Development and evaluation of a convection scheme for use in climate models, *J. Atmos. Sci.*, *56*, 1766–1782, 1999.
- Forster, C., *et al.*, Transport of boreal forest fire emissions from Canada to Europe, *J. Geophys. Res.*, *106*, 22,887–22,906, 2001.
- Forster, C., A. Stohl, P. James, and A. Marenco, The residence times of aircraft emissions in the stratosphere using a mean emission inventory and emissions along actual flight tracks, *J. Geophys. Res.*, *108*, doi:10.1029/2002JD002515, in press, 2003.
- Gottelman, A., and A. H. Sobel, Direct diagnoses of stratosphere-troposphere exchange, *J. Atmos. Sci.*, *57*, 3–16, 2000.
- Gibson, J. K., P. Källberg, S. Uppala, A. Nomura, A. Hernandez, and E. Serrano, *ERA Description, ECMWF Re-Anal. Proj. Rep. Ser.*, vol. 1, 1997.
- Grewe, V., and M. Dameris, Calculating the global mass exchange between stratosphere and troposphere, *Ann. Geophys.*, *14*, 431–442, 1996.
- Hoerling, M. P., T. K. Schaack, and A. J. Lenzen, A global analysis of stratospheric-tropospheric exchange during northern winter, *Mon. Weather Rev.*, *121*, 162–172, 1993.
- Hoinka, K. P., The tropopause: Discovery, definition and demarcation, *Meteorol. Z.*, *6*, 281–303, 1997.
- Holton, J. R., P. H. Haynes, M. E. McIntyre, A. R. Douglass, R. B. Rood, and L. Pfister, Stratosphere-troposphere exchange, *Rev. Geophys.*, *33*, 403–439, 1995.
- James, P., A. Stohl, C. Forster, S. Eckhardt, P. Seibert, and A. Frank, A 15-year climatology of stratosphere-troposphere exchange with a Lagrangian particle dispersion model, 2, Mean climate and seasonal variability, *J. Geophys. Res.*, *108*, doi:10.1029/2002JD002639, in press, 2003.
- Jukes, M. N., The mass flux across the tropopause: Quasigeostrophic theory, *Q. J. R. Meteorol. Soc.*, *123*, 71–99, 1997.
- Jukes, M. N., The descent of tropospheric air into the stratosphere, *Q. J. R. Meteorol. Soc.*, *126*, 319–337, 2000.
- Källberg, P., *Aspects of the Re-Analysed Climate, ECMWF Re-Anal. Proj. Rep. Ser.*, vol. 2, 1997.

- Kowol-Santen, J., H. Elbern, and A. Ebel, Estimation of cross-tropopause air mass fluxes at midlatitudes: Comparison of different numerical methods and meteorological situations, *Mon. Weather Rev.*, *128*, 4045–4057, 2000.
- Meloen, J., et al., Stratosphere-troposphere exchange: A model and method intercomparison, *J. Geophys. Res.*, *108*, doi:10.1029/2002JD002274, in press, 2003.
- Mote, P. W., K. H. Rosenlof, M. E. McIntyre, E. S. Carr, J. C. Gille, J. R. Holton, J. S. Kinnery, H. C. Pumphrey, J. M. Russell, and J. W. Waters, An atmospheric tape recorder: The imprint of tropical tropopause temperatures on stratospheric water vapor, *J. Geophys. Res.*, *101*, 3989–4006, 1996.
- Park, J., M. Ko, C. Jackman, R. Plumb, J. Kaye, and K. Sage (Eds.), *Models and Measurements Intercomparison II, NASA Tech. Publ.*, NASA/TM-1999-209554, pp. 494, 1999.
- Pawson, S., and M. Fiorino, A comparison of reanalyses in the tropical stratosphere, 1, Thermal structure and the annual cycle, *Clim. Dyn.*, *14*, 631–644, 1998a.
- Pawson, S., and M. Fiorino, A comparison of reanalyses in the tropical stratosphere, 2, The quasi-biennial oscillation, *Clim. Dyn.*, *14*, 645–658, 1998b.
- Plumb, R. A., A “tropical pipe” model of stratospheric transport, *J. Geophys. Res.*, *101*, 3957–3972, 1996.
- Reithmeier, C., Untersuchungen zum globalen Spurenstofftransport und Stratosphären-Troposphären-Austausch mit dem Lagrangeschen Modell ECHAM4/ATTLA, Dissertation, Ludwig-Maximilians-Univ. München, Report 2001-09 of the series of Deutsches Zentrum für Luft- und Raumfahrt e.V., Oberpfaffenhofen, 2001.
- Rind, D., J. Lerner, K. Shah, and R. Suozzo, Use of on-line tracers as a diagnostic tool in general circulation model development, 2, Transport between the troposphere and stratosphere, *J. Geophys. Res.*, *104*, 9151–9167, 1999.
- Roelofs, G.-J., and J. Lelieveld, Model study of the influence of cross-tropopause O₃ transports on tropospheric O₃ levels, *Tellus, Ser. B*, *49*, 38–55, 1997.
- Seibert, P., B. Krüger, and A. Frank, Parametrisation of convective mixing in a Lagrangian particle dispersion model, paper presented at Proceedings of the 5th GLOREAM Workshop, Wengen, Switzerland, September 24–26, 2001, 2001.
- Siegmund, P. C., P. F. J. Van Velthoven, and H. Kelder, Cross-tropopause transport in the extra-tropical northern winter hemisphere, diagnosed from high-resolution ECMWF data, *Q. J. R. Meteorol. Soc.*, *122*, 1921–1941, 1996.
- Sprenger, M., and H. Wernli, A northern hemispheric climatology of cross-tropopause exchange for the ERA15 time period (1979–1993), *J. Geophys. Res.*, *108*, doi:10.1029/2002JD002636, in press, 2003.
- Sprenger, M., M. C. Maspoli, and H. Wernli, Tropopause folds and cross-tropopause exchange: A global investigation based upon ECMWF analyses for the time period March 2000 till February 2001, *J. Geophys. Res.*, *108*, doi:10.1029/2002JD002587, in press, 2003.
- Stohl, A., A 1-year Lagrangian “climatology” of airstreams in the Northern Hemisphere troposphere and lowermost stratosphere, *J. Geophys. Res.*, *106*, 7263–7279, 2001.
- Stohl, A., and D. J. Thomson, A density correction for Lagrangian particle dispersion models, *Boundary Layer Meteorol.*, *90*, 155–167, 1999.
- Stohl, A., and T. Trickl, A textbook example of long-range transport: Simultaneous observation of ozone maxima of stratospheric and North American origin in the free troposphere over Europe, *J. Geophys. Res.*, *104*, 30,445–30,462, 1999.
- Stohl, A., M. Hittenberger, and G. Wotawa, Validation of the Lagrangian particle dispersion model FLEXPART against large scale tracer experiment data, *Atmos. Environ.*, *24*, 4245–4264, 1998.
- Stohl, A., N. Spichtinger-Rakowsky, P. Bonasoni, H. Feldmann, M. Memmesheimer, H. E. Scheel, T. Trickl, S. Hübener, W. Ringer, and M. Mandl, The influence of stratospheric intrusions on alpine ozone concentrations, *Atmos. Environ.*, *34*, 1323–1354, 2000.
- Stohl, A., et al., Stratosphere-troposphere exchange: A review and what we have learned from STACCATO, *J. Geophys. Res.*, *108*, doi:10.1029/2002JD002490, in press, 2003.
- Trenberth, K. E., D. P. Stepaniak, J. W. Hurrell, and M. Fiorino, Quality of reanalyses in the tropics, *J. Clim.*, *14*, 1499–1510, 2001.
- Vaughan, G., and C. Timmis, Transport of near-tropopause air into the lower midlatitude stratosphere, *Q. J. R. Meteorol. Soc.*, *124*, 1559–1578, 1998.
- Vogelezang, D. H. P., and A. A. M. Holtslag, Evaluation and model impacts of alternative boundary-layer height formulations, *Boundary Layer Meteorol.*, *81*, 245–269, 1996.
- Waugh, D. W., Seasonal variation of isentropic transport out of the tropical stratosphere, *J. Geophys. Res.*, *101*, 4007–4023, 1996.
- Wei, M.-Y., A new formulation of the exchange of mass and trace constituents between the stratosphere and troposphere, *J. Atmos. Sci.*, *44*, 3079–3086, 1987.
- Wernli, H., and M. Bourqui, A Lagrangian “1-year climatology” of (deep) cross-tropopause exchange in the extratropical Northern Hemisphere, *J. Geophys. Res.*, *107*(D2), 4021, doi:10.1029/2001JD000812, 2002.
- Wernli, H., and H. C. Davies, A Lagrangian-based analysis of extratropical cyclones, 1, The method and some applications, *Q. J. R. Meteorol. Soc.*, *123*, 467–489, 1997.
- Wirth, V., Comments on “A new formulation of the exchange of mass and trace constituents between the stratosphere and troposphere”, *J. Atmos. Sci.*, *52*, 2491–2493, 1995.
- Wirth, V., and J. Egger, Diagnosing extratropical synoptic-scale stratosphere-troposphere exchange: A case study, *Q. J. R. Meteorol. Soc.*, *125*, 635–655, 1999.

S. Eckhardt, C. Forster, P. James, and A. Stohl, Department of Ecology, Technical University of Munich, Am Hochanger 13, D-85354 Freising-Weihenstephan, Germany. (james@forst.tu-muenchen.de)

A. Frank and P. Seibert, Institute of Meteorology and Physics, University of Agricultural Sciences, Vienna, Austria.

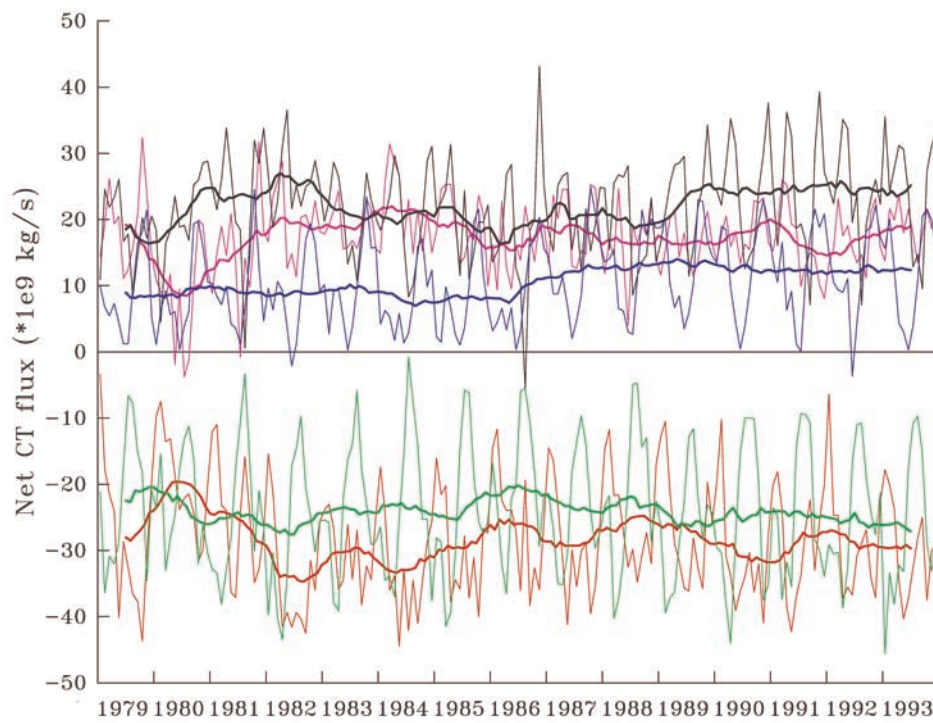


Figure 3. Meridionally integrated monthly mean zonal-mean net cross-tropopause fluxes, units 10^9 kg s^{-1} , with 12-month running means (thicker lines) for 1979 to 1993, averaged over 5 latitude bands: 51°N – 90°N (blue), 21°N – 51°N (green), 21°S – 21°N (black), 51°S – 21°S (red), 90°S – 51°S (violet).